Kinetics of regulated protein–protein interactions revealed with firefly luciferase complementation imaging in cells and living animals

Kathryn E. Luker*, Matthew C. P. Smith*, Gary D. Luker*, Seth T. Gammon*, Helen Piwnica-Worms†‡§, and David Piwnica-Worms*¶‖

*Molecular Imaging Center, Mallinckrodt Institute of Radiology, and Departments of ¶Molecular Biology and Pharmacology, †Cell Biology and Physiology, and ‡Internal Medicine, and §Howard Hughes Medical Institute, Washington University School of Medicine, St. Louis, MO 63110

Communicated by Lewis C. Cantley, Harvard Institutes of Medicine, Boston, MA, June 14, 2004 (received for review March 19, 2004)

Signaling pathways regulating proliferation, differentiation, and apoptosis are commonly mediated through protein–protein interactions as well as reversible phosphorylation of proteins. To facilitate the study of regulated protein–protein interactions in cells and living animals, we optimized firefly luciferase protein fragment complementation by screening incremental truncation libraries of N- and C-terminal fragments of luciferase. Fused to the rapamycin-binding domain (FRB) of the kinase mammalian target of rapamycin and FK506-binding protein 12 (FKBP), respectively, the optimized FRB-N-terminal luciferase fragment (NLuc)/C-terminal luciferase fragment (CLuc)-FKBP luciferase complementation imaging (LCI) pair reconstituted luciferase activity in cells upon single-site binding of rapamycin in an FK506-competitive manner. LCI was used in three independent applications. In mice bearing implants of cells expressing the FRB-NLuc/CLuc-FKBP LCI pair, dose- and time-dependent luciferase activity allowed target-specific pharmacodynamic analysis of rapamycin-induced protein–protein interactions *in vivo*. In cells expressing a Cdc25C-NLuc/CLuc-14-3-3ε LCI pair, drug-mediated disruption of cell cycle regulated protein–protein interactions was demonstrated with the protein kinase inhibitor UCN-01 in a phosphoserine-dependent manner. When applied to IFN-γ-dependent activation of Janus kinase/signal transducer and activator of transcription 1 (STAT1), LCI revealed, in the absence of ligand-induced phosphorylation, STAT1 proteins existing in live cells as preformed dimers. Thus, optimized LCI provides a platform for near real-time detection and characterization of regulated and small molecule-induced protein–protein interactions in intact cells and living animals and should enable a wide range of novel applications in drug discovery, chemical genetics, and proteomics research.

Regulated protein–protein interactions are fundamental to living systems, mediating many cellular functions, including cell cycle progression, signal transduction, and metabolic pathways (1, 2). In cancer, aberrant patterns of protein interactions arise from dysregulated phosphorylation of receptor tyrosine kinases (e.g., EGFR and Erb2/HER2), tumor suppressors (e.g., p53 and PTEN), and targets that mediate downstream signaling in cell proliferation, survival, and growth [e.g., signal transducer and activator of transcription (STAT), mammalian target of rapamycin (mTOR), and PI3K-Akt] (3). Thus, protein kinases and mediated protein–protein interactions comprising the kinome have emerged as important therapeutic targets in cancer and other human diseases (3–6). However, many protein interactions arise from host–cell interactions in tissue-specific pathways that cannot be investigated fully with *in vitro* systems, and thus there is considerable interest in imaging protein–protein interactions noninvasively in their normal physiological context within living animals with positron emission tomography (7, 8) or bioluminescence imaging (9, 10).

Current strategies for detecting protein–protein interactions include activation of transcription, repression of transcription, activation of signal transduction pathways, or reconstitution of a disrupted enzymatic activity (8, 11, 12). In particular, protein fragment complementation depends on division of a monomeric enzyme into two separate components that do not spontaneously reassemble and function (13, 14). Enzyme activity occurs only upon complementation induced by the interaction of fused protein-binding partners or by small molecules (drugs) that induce the interaction of fused proteins (Fig. 1*A*). Of the available complementation strategies, feasibility studies with luciferase complementation have demonstrated the potential to observe protein–protein interactions in living animals (15, 16). However, available firefly luciferase fragments suffer from constitutive activity of the N terminus fragment, whereas the blue-green emission spectrum of *Renilla* luciferase penetrates tissues poorly, thereby precluding general use. Furthermore, coelenterazine, the chromophoric substrate for *Renilla* luciferase, is transported by the multidrug resistance P-glycoprotein (17), complicating applications of *Renilla* luciferase *in vivo*. Thus, no enzyme fragment pair yet has been found that satisfies all criteria for noninvasive analysis of protein–protein interactions and enables interrogation in cell lysates, intact cells, and living animals. Herein, we characterize optimized firefly luciferase complementation imaging (LCI), a robust and broadly applicable bioluminescence approach with applications to both modification-independent and phosphorylation-dependent protein interactions in lysates, cells, and animals.

Methods

Chemicals and Reagents. UCN-01 (NSC 638850) was provided by Jill Johnson (Drug Synthesis and Chemistry Branch, National Cancer Institute, National Institutes of Health, Bethesda). Luciferin was obtained from Xenogen (Alameda, CA). Rapamycin was obtained from Sigma.

Library Construction and Screening. The initial N- and C-terminal fragments of firefly (*Photinus pyralis*) luciferase were amplified from pGL3-Control (Promega). The rapamycin-binding domain (FRB) of human mTOR (residues 2024–2113) and human FK506-binding protein 12 (FKBP) were generated by PCR amplification from plasmids kindly provided by X. F. Zheng (Washington University). A flexible Gly/Ser linker and a multiple cloning site (*Bgl*II, *Bsi*WI, *Mlu*I, and *Sma*I) were added by using synthetic oligonucleotide primers. The fusions were expressed in *Escherichia coli* in plasmids pDIM-N2 and pDIM-C6 (gift of S. Benkovic, Pennsylvania State University, University Park) (18).

N- and C-terminal incremental truncation libraries were con-

Abbreviations: CLuc, C-terminal luciferase fragment; EGFP, enhanced GFP; FKBP, FK506-binding protein 12; FRB, rapamycin-binding domain of mammalian target of rapamycin; IVIS, *in vivo* imaging system; LCI, luciferase complementation imaging; mTOR, mammalian target of rapamycin; NLuc, N-terminal luciferase fragment; STAT, signal transducer and activator of transcription; HEK, human embryonic kidney.

‖To whom correspondence should be addressed. E-mail: piwnica-wormsd@mir.wustl.edu.

www.pnas.org/cgi/doi/10.1073/pnas.0404041101

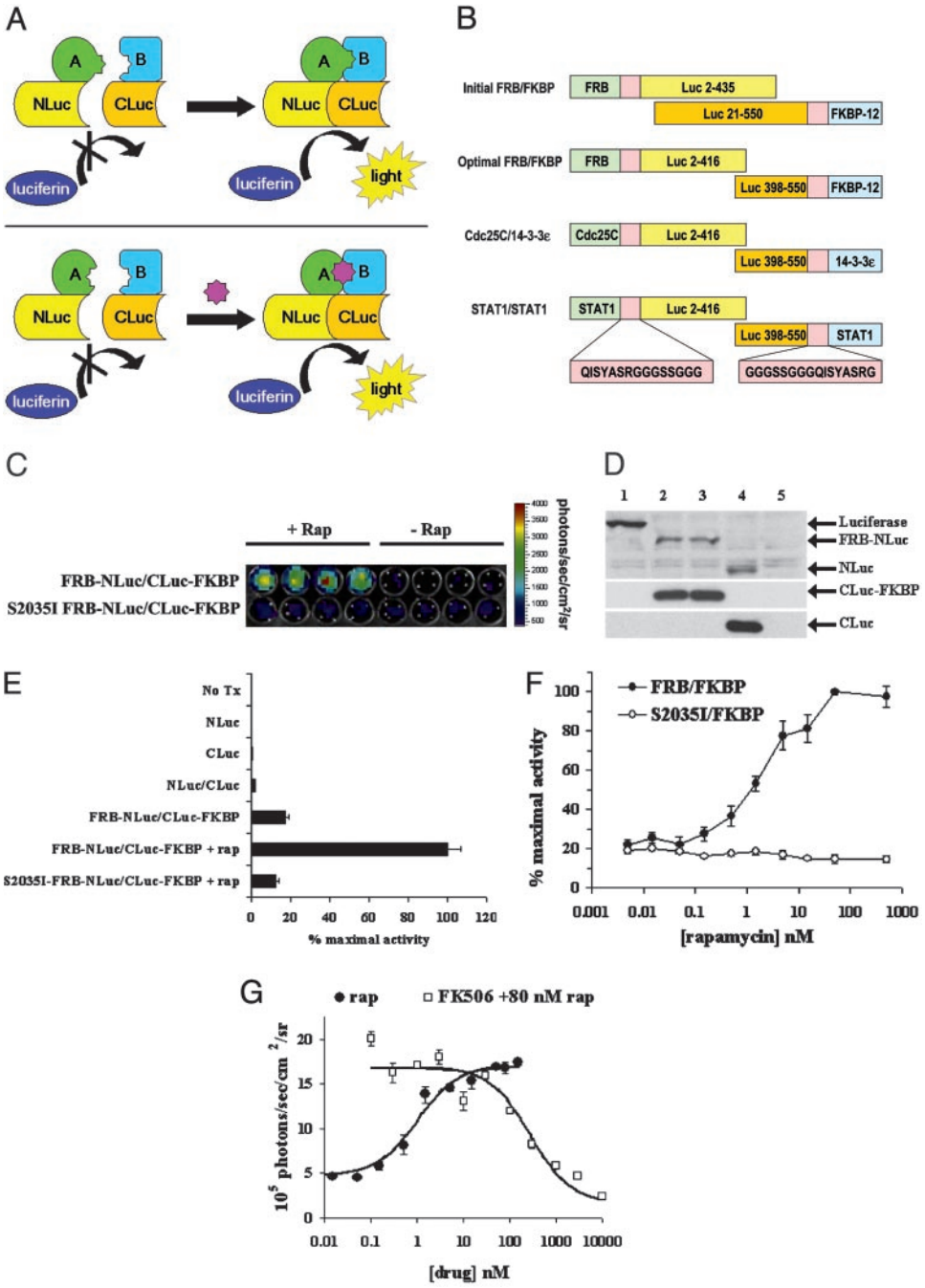

Fig. 1. LCI of induced FRB/FKBP interaction in cells. (*A*) Schematic of LCI. Spontaneous association (*Upper*) or drug-induced association (*Lower*) of proteins A and B bring inactive fragments of luciferase into close proximity to reconstitute bioluminescence activity. (*B*) The initial FRB-NLuc and CLuc-FKBP fusions were used to generate incremental truncation libraries from which the optimal FRB-NLuc/CLuc-FKBP LCI pair was obtained. Additional constructs were generated by replacement of FRB or FKBP with the indicated ORFs. (*C*) Monitoring rapamycin-induced FRB/FKBP association in live cells. HEK-293 cells transfected with FRB-NLuc/CLuc-FKBP or S2035I FRB-NLuc/CLuc-FKBP were treated for 6 h with 50 nM rapamycin. A pseudocolor IVIS bioluminescence image of live cells in a 96-well plate is shown. (*D*) Western blots of whole-cell extracts (100 μg of protein per lane) from untransfected HEK-293 cells (lane 5) or cells transfected with intact luciferase (lane 1), FRB-NLuc/CLuc-FKBP (lane 2), S2035I FRB-NLuc/CLuc-FKBP (lane 3), or unfused NLuc/CLuc (lane 4). Western blots were probed with a polyclonal antiluciferase antibody. (Note that the polyclonal antibody recognizes different epitopes on the NLuc and CLuc fragments so that relative levels of the two fragments cannot be directly assessed.) (*E*) Characterization of FRB-NLuc/CLuc-FKBP LCI in cells. Untransfected HEK-293 cells (no Tx) or cells transfected with various LCI pairs as indicated were treated with vehicle alone or with rapamycin (80 nM) for 6 h before IVIS imaging. Data are expressed as percent of maximal bioluminescence (mean ± SEM of quadruplicate wells). (*F*) Concentration dependence of rapamycin-induced FRB/FKBP association and effect of mutant FRB(S2035I). HEK-293 cells were transfected with FRB-NLuc/CLuc-FKBP or S2035I FRB-NLuc/CLuc-FKBP and treated with various concentrations of rapamycin for 6 h before IVIS imaging. Data are expressed as percent of maximal bioluminescence (mean ± SEM of quadruplicate wells). (*G*) Determination of the apparent K_d of rapamycin-induced as well as K_i of FK506-mediated inhibition of rapamycin-induced FRB/FKBP association in live cells. To assure complete drug permeation, HEK-293 cells transfected with FRB-NLuc/CLuc-FKBP were pretreated 22 h before LCI with the indicated concentrations of rapamycin alone or with rapamycin at the EC_{90} (80 nM) in the presence of the indicated concentrations of FK506. Data, expressed as mean photon flux ± SEM of quadruplicate wells, are representative of three independent experiments.

structed by unidirectional digestion with exonuclease III essentially as described (18). Both libraries were characterized by sequencing and restriction digest of randomly chosen clones to confirm that the obtained truncations covered the full length of each luciferase fragment. Libraries were packaged in phage and *E. coli* were coinfected with phage libraries followed by selection on LB agar plates containing 50 μg/ml ampicillin, 50 μg/ml chloramphenicol, 0.3 mM isopropyl thiogalactopyranoside, and 1 μM rapamycin. To visualize positive clones, colonies were blotted to sterile nitrocellulose filters. Filters were moistened with substrate solution [1 mM D-luciferin in 0.1 M sodium acetate (pH 5.0) for 3–5 min] (19) and then imaged with a charge-coupled device camera [*in vivo* imaging system (IVIS), Xenogen; 1-min exposure; aperture f-stop, 1; binning, 8; field of view, 15 cm] to locate bioluminescent colonies. Clones of interest were isolated and retested for rapamycin-inducible bioluminescence. Plasmids were rescued from these clones, separated, and retransformed into *E. coli* to confirm that plasmid pairs, not single plasmids, recapitulated the original phenotype. The extent of deletion in candidate LCI pairs was characterized by sequencing. Fusions were amplified with primers adding a Kozak consensus sequence to the 5′ end and ligated into mammalian expression vectors pcDNA3.1-V5/HIS TOPO [FRB-N-terminal luciferase fragment (NLuc)] and pEF6-V5/HIS TOPO [C-terminal luciferase fragment (CLuc)-FKBP] (Invitrogen).

DNA Constructs. To replace the FRB with human Cdc25C or human p91 STAT1 (J. E. Darnell, Jr., The Rockefeller University, New York) in the NLuc fusion vector, ORFs of these cDNAs were amplified by PCR by using 5′ primers containing a *Bam*HI site and Kozak consensus sequence upstream of the start site and 3′ primers that reconstituted the linker region up to the *Bsi*WI site. FRB was replaced by using the *Bam*HI and *Bsi*WI sites. FKBP was similarly replaced with human 14-3-3ε or STAT1 by using *Bsi*WI at the 5′ end and *Eco*RV at the 3′ end.

Site-directed mutagenesis (QuikChange, Stratagene) was used to generate point mutations in FRB (S2035I), Cdc25C (S216A), and STAT1 (Y701F) and to introduce a stop codon in CLuc-FKBP at the 3′ end of the linker for expression of unfused CLuc. Unfused NLuc (2–416) was amplified from pGL3 and ligated into pcDNA3.1-V5/HIS TOPO.

The STAT1-NLuc and CLuc-STAT1 ORFs were cloned into lentiviral vectors (gift of J. Milbrandt, Washington University) downstream of a cytomegalovirus promoter and upstream of an internal ribosomal entry sequence linked to enhanced GFP (EGFP) (Clontech) or monomeric red fluorescent protein (R. Tsien, University of California at San Diego, La Jolla), respectively.

Cell Culture. All cell lines were cultured in DMEM (Life Technologies, Grand Island, NY) supplemented with 10% FCS/1% glutamine/0.1% penicillin/streptomycin/0.1% fungizone. For cells transduced with lentiviruses, cells were sorted by flow cytometry for coexpression of EGFP and monomeric red fluorescent protein and maintained in culture after sorting.

Bioluminescence Assays. Cells (3×10^6 per 10-cm dish or 1.5×10^5 per 35-mm dish) were transiently cotransfected with pairs of plasmids or single plasmids as indicated by using FuGENE-6 (Roche, Indianapolis, IN) according to the manufacturer's directions. For bioluminescence assays, transfected cells (1×10^4 per well in 100 μl of medium) were transferred to 96-well black-walled plates 16–24 h after transfection. Subsequently, growth media were replaced with media containing appropriate drugs or vehicle and cells incubated for the times indicated. To image live cells, D-luciferin (10 μl of 1.5 mg/ml in PBS) was added to wells. Photon flux for each well was measured 8–10 min after addition of D-luciferin with an IVIS charge-coupled device camera (1-min exposure; f-stop, 1; binning, 8; field of view, 15 cm).

Whole-cell lysates used for imaging were prepared by using Reporter Lysis Buffer (Promega) according to the manufacturer's directions. For STAT1 studies, cytoplasmic and nuclear extracts were prepared as described (20). For each sample, a 1:5 vol/vol ratio of lysate or extract to Luciferase Assay Reagent (Promega) was added to each well. Bioluminescence was measured immediately by using the IVIS as above, and luminescence was normalized to protein content in samples as determined by bicinchoninic acid (Pierce) or Bradford assay (Bio-Rad, Hercules, CA).

Western Blot Analysis. Cells (3×10^6 per 10-cm dish) were transfected with the indicated plasmids (6 μg each). Treated and untreated cells were washed in PBS, and lysates or extracts were prepared. Whole-cell lysates were prepared in 10 mM Tris (pH 8.5)/1% SDS/1 mM sodium orthovanadate. For studies with Cdc25C, cells were lysed by incubation for 30 min at 4°C with 1 ml of RIPA buffer containing protease inhibitors (21). After centrifugation to remove insoluble material, protein concentration was determined by bicinchoninic acid (Pierce). Proteins were separated by SDS/PAGE and analyzed by using polyclonal primary antibodies for pGL3 luciferase (Promega), phospho-Cdc25C (S216), STAT1 (Santa Cruz Biotechnology), or a monoclonal antibody for phospho-STAT1 (Y701) (Cell Signaling Technology, Beverly, MA). Bound primary antibodies were visualized with horseradish peroxidase-conjugated secondary antibodies by using enhanced chemiluminescence (Amersham Pharmacia).

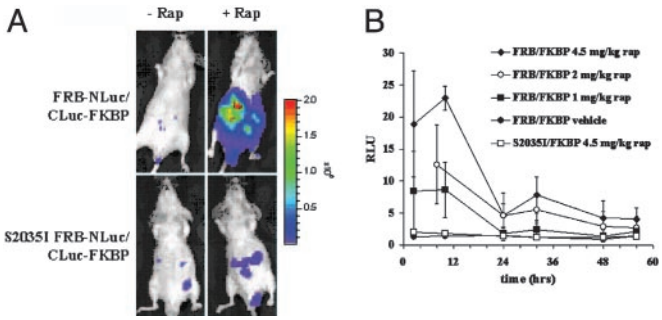

Fig. 2. LCI of induced FRB/FKBP interactions *in vivo*. (*A*) LCI of two representative *nu/nu* mice, one implanted with HEK-293 cells expressing FRB-NLuc/CLuc-FKBP (*Upper*) and the other with cells expressing mutant S2035I FRB-NLuc/CLuc-FKBP (*Lower*). The LCI images were taken 18 h before treatment with rapamycin (*Left*) and 2.5 h after receiving a single dose of rapamycin (4.5 mg/kg, i.p.) (*Right*). (*B*) Monitoring rapamycin-induced FRB/FKBP association in mice by LCI. At the indicated times after treatment with various doses of rapamycin, mice implanted as above were imaged with an IVIS. Data represent the mean ± SEM of four mice in each group imaged repeatedly over the course of the experiment and are expressed relative to background bioluminescence of unimplanted mice (RLU).

Mouse Imaging. Human embryonic kidney (HEK)-293 cells were transfected (6 μg each plasmid per 4×10^6 cells) with FRB-NLuc/CLuc-FKBP or FRB(S2035I)-NLuc/CLuc-FKBP, as indicated. Twenty-four hours after transfection, 2×10^6 cells suspended in 150 μl of Matrigel (BD Biosciences, San Jose, CA) were implanted i.p. into nude mice [male, 6 wk, NCRU-*nu/nu* (Taconic Farms)]. Two hours later, mice were injected with D-luciferin (i.p.; 150 μg/g in PBS) and imaged 10 min later with the IVIS (1-min exposure; binning, 8; f-stop, 1; field of view, 15 cm). After an additional 18 h, groups of four mice were treated with rapamycin (i.p.; 1.0, 2.0, or 4.5 mg/kg) in vehicle (80% DMSO/20% EtOH) or vehicle only. At the indicated times after treatment with rapamycin (Fig. 2*B*), mice were again injected with D-luciferin (i.p.) and imaged 10 min later. Photon flux (photons per second per cm^2 per steradian) was quantified on images by using a uniform rectangular region of interest encompassing the entire abdomen and analyzed with LIVINGIMAGE (Xenogen) and IGOR (Wavemetrics, Lake Oswego, OR) image analysis software.

Results

The Ser-Thr kinase mTOR is inhibited by FKBP in a rapamycin-dependent manner (22). We chose FRB, the 11-kDa domain of human mTOR that binds with high affinity to the rapamycin–FKBP complex, to construct and screen a comprehensive incremental truncation library for optimized LCI. ORFs for FRB and FKBP were fused in frame with overlapping inactive N and C fragments of firefly (*P. pyralis*) luciferase (15, 23), respectively (Fig. 1*B*). From these constructs, N- and C-terminal incremental truncation libraries were generated by unidirectional exonuclease digestion and validated for coverage of all possible deletions essentially as described (18). The FRB-NLuc and CLuc-FKBP incremental truncation libraries were then coexpressed in *E. coli* in the presence of rapamycin to identify pairs of luciferase fragments reconstituting bioluminescence. Of the ≈19,000 colonies screened, 123 (0.65%) produced significant bioluminescence (>10-fold over background). Of these, three truncation pairs emerged displaying the strongest rapamycin-inducible increase in bioluminescence in *E. coli*. Notably, the three optimal LCI pairs contained ORFs that were highly conserved (NLuc/CLuc combinations of amino acids 2-416/398-550, 2-422/396-550, and 2-432/396-550).

Rapamycin-Induced Association of FRB and FKBP. When expressed transiently in HEK-293 cells, the LCI pair with optimal perfor-

mance and minimal overlap [FRB-NLuc(2-416)/CLuc (398–550)-FKBP (Fig. 1*B*), hereafter referred to as FRB-NLuc/CLuc-FKBP] produced strong rapamycin-induced bioluminescence (Fig. 1*C*). Expression of FRB-NLuc and CLuc-FKBP was confirmed by Western blot by using antiluciferase antibody (Fig. 1*D*). Under optimal transient transfection conditions in HEK-293 cells (33 ng of DNA each in a 1:1 ratio), FRB-NLuc/CLuc-FKBP plus rapamycin produced a maximal bioluminescence of 2×10^6 photon flux units/1×10^4 cells in a 96-well format (7×10^4 photon flux units per μg of protein), 1,200-fold greater than untransfected cells or blank wells (Fig. 1*E*). By comparison, a control plasmid (pGL3) expressing intact luciferase produced 3-fold greater bioluminescence (6×10^6 photon flux units/1×10^4 cells transfected with 33 ng of DNA). Rapamycin increased bioluminescence in a dose- and time-dependent manner in live cells transfected with the FRB-NLuc/CLuc-FKBP LCI pair, reaching a maximum of 6-fold induction 4–6 h after addition of drug (Fig. 1 *E* and *F*). To eliminate the effect of membrane permeability of rapamycin on the induction of bioluminescence, rapamycin also was added directly to whole-cell lysates of cells transfected with identical LCI constructs. In these lysates, we observed rapid ($t_{1/2} < 1$ min) and robust (18-fold) induction of bioluminescence by rapamycin (80 nM). Therefore, the kinetics and maximal induction of bioluminescence observed in intact cells were likely an accurate measure of the membrane-specific permeation kinetics of rapamycin into cells and not an inherent performance limitation of the LCI reporter system.

Induction of bioluminescence by rapamycin was saturable and specific in intact HEK-293 cells coexpressing the FRB-NLuc/CLuc-FKBP LCI pair. Displaying single-site rapamycin binding with an apparent K_d of 1.5 ± 0.3 nM ($n = 3$) (Fig. 1*G*), LCI compared favorably with previously reported FRB-FKBP colorimetric and fluorescence-based complementation systems (24, 25). FK506, a competitive inhibitor of rapamycin binding to FKBP (25, 26), inhibited rapamycin-induced luciferase activity *in situ* with an apparent K_i of 4.2 nM (average value; $n = 2$) (Fig. 1*G*). Furthermore, the S2035I mutation of mTOR is known to abrogate rapamycin-induced association of FKBP with FRB (26). Herein, the S2035I FRB-NLuc/CLuc-FKBP LCI pair produced low rapamycin-insensitive luciferase activity in live cells similar to FRB-NLuc/CLuc-FKBP in the absence of rapamycin (Fig. 1 *C*, *E*, and *F*), consistent with the previously described weak rapamycin-independent association of FRB and FKBP (25, 26). Expression levels of the S2035I FRB-NLuc/CLuc-FKBP pair were identical to FRB-NLuc/CLuc-FKBP as assessed by Western blotting (Fig. 1*D*).

To characterize background bioluminescence, we transfected cells with individual fusion constructs as well as an unfused NLuc/CLuc pair. Individual fusion constructs produced no detectable bioluminescence relative to untransfected cells in both HEK-293 and -293T cells under maximal transfection conditions (Fig. 1*E* and data not shown), a significant improvement over the activity of N-terminal fragments of firefly luciferase in previously described split enzyme reporters based on naturally occurring domains of luciferase (10, 15). In cells expressing a pair of unfused NLuc and CLuc fragments, dim bioluminescence was observed (Fig. 1*E*). This background due to self association of the luciferase fragments per se was 12-fold less than the FRB-NLuc/CLuc-FKBP LCI pair in the absence of rapamycin and 100-fold less than the specific signal obtained for the FRB-NLuc/CLuc-FKBP fusion pair in the presence of rapamycin. Western blotting confirmed similar expression levels for all unfused and corresponding fused luciferase fragments (Fig. 1*D*). Overall, these data indicated that the bioluminescence output of this LCI system was dominated by association of the interacting proteins. Furthermore, the quantitative pharmacological titration of rapamycin strongly suggested that the overall free energy contribution of luciferase fragment folding was effectively zero (27).

We next applied LCI to pharmacodynamic analysis of rapamycin-induced protein–protein interactions in living mice. We measured

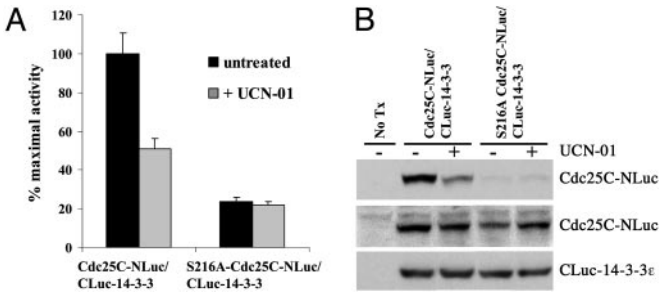

Fig. 3. LCI of phosphoserine-specific interactions of Cdc25C and 14-3-3ε in cells. (*A*) HEK-293 cells transfected with Cdc25C-NLuc/CLuc-14-3-3ε or mutant S216A Cdc25C-NLuc/CLuc-14-3-3ε were treated with vehicle alone or UCN-01 (1 μM) for 6 h before LCI. Data are expressed as percent of bioluminescence relative to untreated Cdc25C-NLuc/CLuc-14-3-3ε cells and represent the mean ± SEM of three independent experiments, $n = 4$ each. (*B*) Western blots of untransfected HEK-293 cells (no Tx) or cells transfected with Cdc25C-NLuc/CLuc-14-3-3ε or S216A Cdc25C-NLuc/CLuc-14-3-3ε. Cells were left untreated or were treated with UCN-01 (1 μM) for 6 h before lysis, processed, and then probed with anti-phospho Cdc25C S216 (*Top*) or anti-luciferase (*Middle* and *Bottom*).

luciferase activity in mice with i.p. implants of cells expressing FRB-NLuc/CLuc-FKBP LCI pairs (Fig. 2). In the absence of rapamycin, bioluminescence in implanted mice did not differ from unimplanted mice. Mice treated with a single administration of rapamycin at a dose sufficient to produce antiangiogenic and antitumor effects (i.p.; 1.0, 2.0, or 4.5 mg/kg) (28) showed dose-dependent increases in bioluminescence with a maximum signal of 23-fold over untreated mice. Induction of bioluminescence by a single dose of rapamycin was maximal 2.5 h after treatment, remained high for 10 h, and then decreased by 24 h to a low steady state of ≈25% of maximum. In contrast, mice implanted with cells expressing mutant S2035I FRB-NLuc/CLuc-FKBP showed no detectable signal over background and no response to rapamycin. Interestingly, the kinetics and fold induction of bioluminescence produced by rapamycin in mouse peritoneal HEK-293 cell implants was similar to cell lysates, and both were more rapid and of greater magnitude than for identically transfected HEK-293 cells in tissue culture. Therefore, it seems likely that the pharmacokinetics and cell permeation properties of rapamycin are enhanced *in situ* in the living animal. LCI produced strong specific bioluminescence that could be used to repetitively quantify and spatially localize target proteins of interest in a dose- and time-dependent manner in living mice.

Association of Cdc25C with 14-3-3ε. Next LCI was used to monitor the phosphorylation-dependent interactions between human Cdc25C with 14-3-3ε. Cdc25C is a protein phosphatase that positively regulates the cell division cycle by activating cyclin-dependent protein kinases (29). Perturbation of the Cdc25C/14-3-3 regulatory pathway causes partial abrogation of the DNA replication and DNA damage checkpoints (30). The staurosporine analog UCN-01, a protein kinase inhibitor in phase II clinical trials for cancer treatment, inhibits protein kinases that phosphorylate Cdc25C on S216, thereby diminishing 14-3-3ε binding to Cdc25C (21). In HEK-293 cells coexpressing a Cdc25C-NLuc/CLuc-14-3-3ε LCI pair (Fig. 1*B*), a maximum signal of 1.4×10^6 photon flux units/1×10^4 cells in a 96-well format was obtained (defined as 100% activity) (Fig. 3*A*). This indicated a productive interaction between the Cdc25C and 14-3-3ε fusion proteins. Importantly, the S216A mutation abrogates 14-3-3ε binding to Cdc25C (30) and substantially reduced bioluminescence output (Fig. 3*A*), confirming specificity of the LCI signal. Furthermore, UCN-01 decreased bioluminescence (Fig. 3*A*), correlating with a reduction in phosphorylation of Cdc25C-NLuc on S216 (Fig. 3*B*, lanes 2 and 3). Thus, LCI monitored noninvasively within living cells the activity of protein kinase

MEDICAL SCIENCES

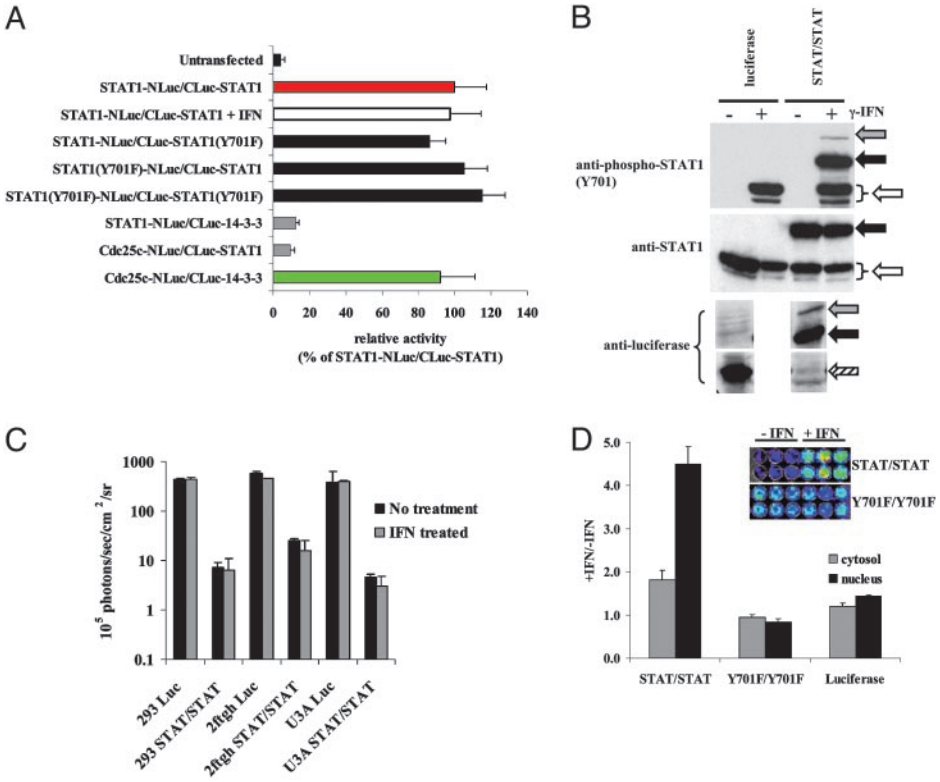

Fig. 4. Characterization of STAT1-NLuc/CLuc-STAT1 LCI in live cells. (*A*) Untransfected HEK-293 cells or cells transfected with various LCI pairs are indicated. Cellular STAT1/STAT1 pairs were untreated (red bar) or treated with IFN-γ (1,000 units/ml) for 30 min (unfilled bar) before IVIS imaging. Y701F mutant STAT1 was expressed with wild-type STAT1 or as a mutant pair (black bars). STAT1 fusions were also mismatched with Cdc25C or 14-3-3ε fusions (gray bars). The interacting pair Cdc25C-NLuc/CLuc-14-3-3ε (green bar) is included as a positive control. Data are expressed as percent of STAT1-NLuc/CLuc-STAT1 bioluminescence and represent the mean ± SEM ($n = 4$) of a representative experiment. (*B*) Western blots of whole-cell lysates of HEK-293 cells cotransduced with STAT1-NLuc/CLuc-STAT1 lentiviruses or singly transduced with a luciferase lentivirus. Cells were left untreated or treated with IFN-γ (1,000 units/ml) for 30 min before lysis, processed for Western analysis and then probed with the antibodies indicated to visualize expression and IFN-γ-induced phosphorylation of STAT1-NLuc (gray arrows), CLuc-STAT1 (black arrows), and endogenous p91 and p84 STAT1 (unfilled arrows). Intact luciferase expression (hatched arrow) is also shown. Note that whereas STAT1-NLuc could not be visualized using the STAT1 antibody, the fusion could be visualized with both Luc and phospho-STAT1 antibodies. (*C*) Effect of IFN-γ on bioluminescence of intact cells (HEK-293, 2ftgh, and U3A) transduced with lentiviral constructs expressing STAT1-NLuc/CLuc-STAT1 (STAT/STAT) or intact luciferase (Luc). Each transduced cell line was sorted by fluorescence-activated cell sorting for expression of appropriate fluorescence markers (EGFP and monomeric red fluorescent protein). These enriched populations were seeded in a 96-well format (10^4 cells per well) and left untreated or treated with IFN-γ (1,000 units/ml for 30 min). Bars represent the mean ± SEM ($n = 4$) for a representative experiment. Note the *y* axis log scale. (*D*) Dependence of bioluminescence of cytoplasmic and nuclear extracts on IFN-γ treatment. HEK-293 cells were transiently transfected with STAT1-NLuc/CLuc-STAT1, the Y701F STAT1 mutant LCI pair, or intact luciferase. Forty-eight hours after transfection, cells were left untreated or treated with IFN-γ (1,000 units/ml for 20 min) ($n = 3$ for each) and then extracts prepared. To measure bioluminescence in extracts, an assay buffer including D-luciferin and ATP (Luciferase Assay Buffer, Promega) was added to duplicate samples of each extract. Bars show the ratio ± SEM of mean photon flux per μg of protein for extracts of IFN-γ treated over untreated cells. (*Inset*) Raw bioluminescence data for nuclear extracts of cells transfected with the indicated pairs. Duplicate determinations are vertically arranged with independent extracts arrayed horizontally.

inhibitors known to block phosphorylation-dependent protein–protein interactions.

STAT1 Homodimerization. STAT transcription factors are activated by Janus kinase 1-mediated phosphorylation on Y701 in response to IFN-γ (31) and are thought to signal through phosphorylation-dependent dimerization of STAT proteins with subsequent translocation of the active dimer to the nucleus (31). However, several recent studies have suggested the existence of a nonphosphorylated pool of STAT dimers (32–35). We applied LCI to directly test for preassociation of nonphosphorylated homodimers of p91 STAT1 in intact cells. Initial experiments showed that the STAT1-NLuc/CLuc-STAT1 LCI pair produced strong IFN-γ-independent bioluminescence in HEK-293 cells that was specific for the matched STAT1 LCI pair and not observed with mismatched STAT1 LCI pairs (Fig. 4*A*). In addition, Y701F mutation of the STAT1 reporters resulted in bioluminescence identical to cells transfected with wild-type STAT1 reporters, whether these were expressed as homodimeric mutant pairs or as heterodimers with wild-type STAT1 fusions (Fig. 4*A*). STAT1 fusions mismatched with Cdc25C-NLuc or CLuc-14-3-3ε (Fig. 4*A*) or mismatched with FRB-NLuc, CLuc-FKBP, NLuc, or CLuc (data not shown) showed low bioluminescence, confirming specificity of the STAT1 homodimeric signal.

Several possible explanations existed for the persistent bioluminescence of the STAT1 LCI pair. These included constitutive association of unphosphorylated STAT1 reporters, constitutive phosphorylation-dependent association, lack of phosphorylation due to competition by endogenous STATs for Janus kinase 1 (JAK1), or inability of JAK1 to recognize one or both of the reporter proteins due to steric bulk of the fused luciferase fragments. For further analysis, we constructed separate lentiviruses expressing STAT1-NLuc or CLuc-STAT1 fusions driven by cytomegalovirus promoters and coexpressing EGFP or monomeric red fluorescent protein from an internal ribosomal entry sequence, respectively. HEK-293 cells were infected with STAT1 LCI viral pairs and then sorted by fluorescence-activated cell sorting to enrich for cotransduced cells. Similarly, HEK-293 cells infected with a control EGFP-tagged lentivirus encoding intact firefly luciferase were sorted and enriched. Sorted but untreated transfectants showed high bioluminescence, and Western blotting confirmed expression of both STAT1-NLuc and CLuc-STAT1 proteins, each unphosphorylated on Y701 (Fig. 4 *B* and *C*). Treatment with IFN-γ resulted in phosphorylation of both STAT1-NLuc and CLuc-STAT1 as well as endogenous p91 and p84 STAT1 (Fig. 4*B*).

To investigate competition from endogenous STAT1, we similarly cotransduced and sorted a STAT1-deficient cell line, U3A, and its parental 2ftgh fibrosarcoma cell line (36). Although the sorted cell populations showed different levels of constitutive bioluminescence, all cotransduced cells failed to change bioluminescence upon treatment with IFN-γ at any time or at any dose (Fig. 4*C*). Western blots of transduced and sorted U3A and 2ftgh cells were similar in all respects to those shown in Fig. 4*B* for HEK-293 cells and confirmed the absence of endogenous STAT1 in U3A cells (data not shown). Thus, the failure of IFN-γ to induce an increase in

bioluminescence of the STAT1-NLuc/CLuc-STAT1 pair could not be attributed to competitive inhibition by endogenous STAT1.

Finally, to confirm that phosphorylated STAT1 LCI pairs were biologically functional, we measured the IFN-γ-inducible nuclear accumulation of bioluminescence activity. Cytoplasmic and nuclear extracts were prepared from untreated and IFN-γ-treated HEK-293 cells transiently cotransfected with the STAT1-NLuc/CLuc-STAT1 LCI pair, the Y701F mutant pair, or intact luciferase. Bioluminescence (photon flux per μg of protein) was specifically increased in nuclear extracts prepared from IFN-γ-treated cells (20 min, 100 units/ml) (Fig. 4*D*). No such IFN-γ-induced increase in nuclear bioluminescence was observed in extracts of cells transfected with the mutant STAT1 LCI pair or intact luciferase. In similar experiments, U3A cells cotransduced with the STAT1-NLuc/CLuc-STAT1 LCI pair also showed a 6-fold increase ($n = 3$) in bioluminescence of nuclear extracts (photon flux per μg of protein) upon treatment with IFN-γ (30 min, 100 units/ml). Western blots of the cytoplasmic and nuclear extracts used in Fig. 4*D* confirmed purity of the extracts, neither fraction showing crosscontamination as assessed by the marker proteins β-tubulin (cytoplasm) and Topo II (nucleus), respectively (data not shown). Western blots also confirmed virtually identical expression levels of wild-type and Y701F mutant LCI pairs as well as appropriate phosphorylation of STAT1 proteins and reporters (data not shown).

Therefore, these data showed that the STAT1-NLuc/CLuc-STAT1 LCI pair associated constitutively and specifically in live cells and was appropriately phosphorylated in response to IFN-γ treatment, and that bioluminescent dimers translocated to the nucleus in an IFN-γ-dependent manner. Although it is well known that Y701 phosphorylation stabilizes STAT1 homodimers (37), we propose that the behavior of the STAT1 LCI reporter reflected a lower-affinity constitutive association of STAT1 that was stabilized and translocated upon Y701 phosphorylation without altering the total pool of low- and high-affinity STAT1 homodimers.

Discussion

LCI could detect and quantify regulated protein interactions both in live cells and in whole animals with strong and specific induction of bioluminescence. Once synthesized, LCI hybrid proteins form a complete assay system independent of cell-specific molecular complexes, such as the transcriptional machinery required for readout with two-hybrid strategies (8), and thus protein interactions may be detectable in any subcellular compartment in near real time. Protein fragment complementation strategies based on reconstituting active enzymes also offer the potential benefit of signal amplification to enhance sensitivity for detecting weaker interacting proteins (8). Herein, the dynamic range of optimized LCI was robust, with drug-specific induction of bioluminescence reaching 1,200-fold over background, exceeding currently available systems. This property enabled lower-affinity protein–protein interactions, such as nonphosphorylated STAT1 homodimers, to be characterized in their native state in living cells and may broaden the dynamic range of proteomic studies compared to conventional methods.

The crystal structure of luciferase shows two essentially independent folding domains, the N-terminal domain consisting of residues 1–436 and a C-terminal domain of residues 440–550, connected by a disordered flexible region (38). Interestingly, our genetic screen selected an LCI pair for productive activity that fulfilled many criteria of complementary fragments derived from rational protein design applied to other enzymes (27). The optimized LCI pair deleted key structural and active site regions from the N-terminal fragment and, in effect, transferred these regions to the C-terminal fragment (38). The NLuc fragment would be unlikely to adopt an entirely native fold because the core of a β-barrel subdomain is missing, including β-strands C5 and C6 (residues 418–437) containing several invariant and highly conserved residues of the putative active site. Upon interaction, the CLuc fragment would complement the missing subdomains in the NLuc fragment.

Although optimized LCI appears to be broadly adaptable, steric constraints of the system remain to be fully explored. Herein, LCI applications to drug-induced association of heterodimeric complexes (FRB/FKBP), phospho-dependent association of heterodimeric complexes (Cdc25C/14-3-3ε), and ligand-induced translocation of homodimeric complexes (STAT1/STAT1) demonstrated high sensitivity to regulation at the posttranslational level *in situ* and *in vitro*. LCI showed no background bioluminescence arising from individual LCI fragments and minimal bioluminescence arising from unregulated association of the firefly luciferase fragments themselves. Thus, this LCI system may finally prove useful for assessing interactions of proteins in live animals in the context of normal function and disease. Optimized LCI provides a promising tool for high-throughput screening, direct and indirect quantification of drug binding to specific protein targets, and noninvasively characterizing mechanisms of therapeutic response in living organisms.

This work was funded by National Institutes of Health Grant P50 CA94056 and a Siteman Cancer Center Award. H.P.-W. is an investigator of the Howard Hughes Medical Institute.

1. Newton, A. (2003) *Biochem. J.* **370,** 361–371.
2. Ogawa, H., Ishiguro, S., Gaubatz, S., Livingston, D. & Nakatani, Y. (2002) *Science* **296,** 1132–1136.
3. Luo, J., Manning, B. & Cantley, L. (2003) *Cancer Cell* **4,** 257–262.
4. Heldin, C. (2001) *Stem Cells* **19,** 295–303.
5. Darnell, J. E., Jr. (2002) *Nat. Rev. Cancer* **2,** 740–749.
6. Manning, G., Whyte, D., Martinez, R., Hunter, T. & Sudarsanam, S. (2002) *Science* **298,** 1912–1934.
7. Luker, G., Sharma, V., Pica, C., Dahlheimer, J., Li, W., Ochesky, J., Ryan, C., Piwnica-Worms, H. & Piwnica-Worms, D. (2002) *Proc. Natl. Acad. Sci. USA* **99,** 6961–6966.
8. Luker, G., Sharma, V. & Piwnica-Worms, D. (2003) *Methods* **29,** 110–122.
9. Ray, P., Pimenta, H., Paulmurugan, R., Berger, F., Phelps, M., Iyer, M. & Gambhir, S. (2002) *Proc. Natl. Acad. Sci. USA* **99,** 2105–3110.
10. Paulmurugan, R., Umezawa, Y. & Gambhir, S. S. (2002) *Proc. Natl. Acad. Sci. USA* **99,** 15608–15613.
11. Toby, G. & Golemis, E. (2001) *Methods* **24,** 201–217.
12. Lievens, S., Heyden, J., Vertenten, E., Plum, J., Vandekerckhove, J. & Tavernier, J. (2004) *Methods Mol. Biol.* **263,** 293–310.
13. Rossi, F., Charlton, C. & Blau, H. (1997) *Proc. Natl. Acad. Sci. USA* **94,** 8405–8410.
14. Remy, I., Galarneau, A. & Michnick, S. W. (2002) *Methods Mol. Biol.* **185,** 447–459.
15. Ozawa, T., Kaihara, A., Sato, M., Tachihara, K. & Umezawa, Y. (2001) *Anal. Chem.* **73,** 2516–2521.
16. Paulmurugan, R. & Gambhir, S. (2003) *Anal. Chem.* **75,** 1584–1589.
17. Pichler, A., Prior, J. & Piwnica-Worms, D. (2004) *Proc. Natl. Acad. Sci. USA* **101,** 1702–1707.
18. Ostermeier, M., Nixon, A., Shim, J. & Benkovic, S. (1999) *Proc. Natl. Acad. Sci. USA* **96,** 3562–3567.
19. Cebolla, A., Vazquez, M. & Palomares, A. (1995) *Appl. Environ. Microbiol.* **61,** 660–668.
20. Weber-Nordt, R., Riley, J., Greenlund, A., Moore, K., Darnell, J. & Schreiber, R. (1996) *J. Biol. Chem.* **271,** 27954–27961.
21. Graves, P., Yu, L., Schwarz, J., Gales, J., Sausville, E., O'Connor, P. & Piwnica-Worms, H. (2000) *J. Biol. Chem.* **275,** 5600–5605.
22. Harris, T. & Lawrence, J. (2003) *Science STKE* **212,** re15.
23. Sung, D. & Kang, H. (1998) *Photochem. Photobiol.* **68,** 749–753.
24. Galarneau, A., Primeau, M., Trudeau, L.-E. & Michnick, S. (2002) *Nat. Biotechnol.* **20,** 619–622.
25. Remy, I. & Michnick, S. (1999) *Proc. Natl. Acad. Sci. USA* **96,** 5394–5399.
26. Chen, J., Zheng, X., Brown, E. & Schreiber, S. (1995) *Proc. Natl. Acad. Sci. USA* **92,** 4947–4951.
27. Michnick, S. W. (2001) *Curr. Opin. Struct. Biol.* **11,** 472–477.
28. Guba, M., von Breitenbuch, P., Steinbauer, M., Koehl, G., Flegel, S., Hornung, M., Bruns, C. J., Zuelke, C., Farkas, S., Anthuber, M., *et al.* (2002) *Nat. Med.* **8,** 128–135.
29. Nilsson, I. & Hoffmann, I. (2000) *Prog. Cell Cycle Res.* **4,** 107–114.
30. Peng, C., Graves, P., Thoma, R., Wu, Z., Shaw, A. & Piwnica-Worms, H. (1997) *Science* **277,** 1501–1505.
31. Levy, D. E. & Darnell, J. E., Jr. (2002) *Nat. Rev. Mol. Cell Biol.* **3,** 651–662.
32. Stancato, L. F., David, M., CarterSu, C., Larner, A. C. & Pratt, W. B. (1996) *J. Biol. Chem.* **271,** 4134–4137.
33. Braunstein, J., Brutsaert, S., Olson, R. & Schindler, C. (2003) *J. Biol. Chem.* **278,** 34133–34140.
34. Kretzschmar, A. K., Dinger, M. C., Henze, C., Brocke-Heidrich, K. & Horn, F. (2004) *Biochem. J.* **377,** 289–297.
35. Ota, N., Brett, T. J., Murphy, T. L., Fremont, D. H. & Murphy, K. M. (2004) *Nat. Immunol.* **5,** 208–215.
36. Mckendry, R., John, J., Flavell, D., Muller, M., Kerr, I. M. & Stark, G. R. (1991) *Proc. Natl. Acad. Sci. USA* **88,** 11455–11459.
37. Shuai, K., Horvath, C. M., Huang, L. H. T., Qureshi, S. A., Cowburn, D. & Darnell, J. E. (1994) *Cell* **76,** 821–828.
38. Conti, E., Franks, N. P. & Brick, P. (1996) *Structure (London)* **4,** 287–298.